A Game Theory Approach to Energy Management of An Engine-Generator/Battery/Ultracapacitor Hybrid Energy System

He Yin, *Student Member, IEEE*, Chen Zhao, *Student Member, IEEE*, Mian Li, Chengbin Ma, *Member, IEEE*, Mo-Yuen Chow, *Fellow, IEEE*

***Abstract*—The complex configuration and behavior of multi-source hybrid energy systems (HESs) present challenges to their energy management. For a balanced solution, it is especially important to represent and take advantage of the characteristics of each device, and the interactive relationship among them. In this paper multi-agent modeling and a game theory-based control strategy are proposed and combined for the energy management of an example engine-generator/battery/ultracapacitor HES. The three devices, engine-generator unit, battery and ultracapacitor packs, are modeled and controlled as independent but related agents, through which the performance and requirements of the individual devices are fully respected. The energy management problem is then formulated as a non-cooperative current control game. The Nash equilibrium is analytically derived as a balanced solution that compromises the different preferences of the independent devices. The following simulation and experimental results validate the game theory-based control and its real-time implementation. The proposed approach could be further extended to become a general solution for the energy management and control of networked energy systems, in which again fully representing and balancing the different preferences of the components are important.**

***Index Terms*—Hybrid energy system, multi-agent, game theory, engine-generator, battery, ultracapacitor.**

I. Introduction

THE combination of batteries and ultracapacitors (UCs), i.e., a hybrid energy system (HES), has been intensively investigated in recent years [1]–[3]. However, due to the limited energy density of batteries, the battery/UC HES is still incapable of supplying sufficient energy for long-term applications. Further combination with an engine-generator unit, i.e., a three-source HES, has proved to be a feasible solution. Several strategies have been proposed for the energy management of the HESs involving engines, especially for the applications in hybrid electric vehicle (HEV). The power-flow control of a four-wheel-drive series HEV is discussed in [4]. The HEV uses a diesel-engine-generator unit, a lead-acid battery pack, and an UC pack. Control sequences for "normal" and "EV" (electric vehicle) modes were developed. The engine-generator unit only operates in the "normal" mode and becomes idle during deceleration. A "power assistance" mode is further added, in which battery pack provides power to assist the engine and UC pack covers the rest of the load power. The UC pack is charged by the engine-generator unit only when its voltage is lower than a specific value. Besides, the fuel economy was not focused on because of the specific purpose of the target application. [5] explains the concept of a multiple-input DC-DC power converter (MIPEC) for combining power flow from multiple energy sources, and a relatively straightforward strategy was applied for the power-flow control. In the strategy the regenerative fuel cell generator, a main energy source as same as the engine-generator unit, is shut off when the power consumption is less than 20% of its rated value, while the target battery current is constant. The UC current is jointly determined by the UC state-of-charge (SOC) level and the difference between the total load current request and the current supplied by the other two energy sources. [6] gives an overview of the on-board HESs and their control strategies (rule- and optimization-based ones) for HEVs such as a series HEV, in which the engine-generator unit, battery and UC packs are included. As to the control of the three-source HES, the basic consideration is briefly described as operating the engine at its maximum efficiency point through dynamically charging and discharging the battery and UC packs. However, no further details are provided. A review on the control strategies for plug-in HEVs can be found in [7]. Again the rule- and optimization-based strategies, and their implementation are discussed and compared for the on-board engine-generator/battery HES. Adding an UC pack into the HES obviously complicates the interactions within the HES, and requires a comprehensive discussion on modeling and control strategy. [8] presents an energy management strategy that optimizes the engine efficiency and transients for a series engine-generator/battery hybrid powertrain, i.e., again a two-source HES. A model predictive control (MPC) algorithm was developed and implemented to smoothen the engine transients by using the battery, thereby improving efficiency. Meanwhile, ideally in the engine-generator/battery/UC HES it is desirable to operate the engine at its maximum efficiency point (i.e., constant output power of the engine-generator unit), and the battery pack supplies the rest of the average

Manuscript received May 28, 2015; revised October 6, 2015 and December 17, 2015; accepted January 26, 2016. This work was supported in part by the National Natural Science Foundation of China under Grant 51375299 (2014-2017) and 51375302 (2014-2017).

H. Yin, C. Zhao, M. Li, and C. Ma are with the University of Michigan-Shanghai Jiao Tong University Joint Institute, Shanghai Jiao Tong University, 800 Dongchuan Road, Minhang, Shanghai 200240, P. R. China (e-mail: yyy@sjtu.edu.cn; zc437041363@sjtu.edu.cn; mianli@sjtu.edu.cn; chbma@sjtu.edu.cn). M. Li and C. Ma are also with a joint faculty appointment in School of Mechanical Engineering, Shanghai Jiao Tong University.

M.-Y. Chow is with the Department of Electrical and Computer Engineering, North Carolina State University, Raleigh, NC 27695, USA (e-mail: chow@ncsu.edu).

constant load demand (ALD); while the UC pack covers the entire dynamic load. Without considering physical limitations such as in size and weight, this ideal ALD-based control has been theoretically approved to be the most optimal energy management strategy for the HESs [9], [10]. However, in practice besides the physical limitations, an exact prediction of the future load demand is also very difficult, if not impossible. This disadvantage significantly limits the applicability of the ALD-based control because the ALD of the entire test cycle is usually unknown in advance. In the following sections the ALD-based control serves as an ideal case, i.e., a baseline, for comparison purposes.

It is interesting to note that in a HES besides the unique characteristics of each energy source, there are obvious differences in their respective preferences. For example, in the engine-generator/battery/UC HES, the engine-generator unit is a device that is capable of providing long-term energy supply, but its energy efficiency is among the lowest, usually less than 30%, and thus significantly affects the overall efficiency of the final HES [8]. Therefore, in the energy management the preference of the engine-generator unit should be minimizing its fuel consumption as much as possible. On the other hand, the battery pack is more "sensitive" than the UC pack. It has higher energy density, but its cycle life is limited and largely affected by factors such as charging/discharging rate and temperature [11]. Thus for the battery pack the extension of its own cycle life should be given high priority. While the UC pack is a "robust" device that can provide fast and efficient energy delivery and has a long cycle life [12]. However, the limited energy density of the UC pack makes it only suitable to work as an assistive energy storage device. In the HES UC pack plays a crucial role in improving the overall system performance. It is important that the UC pack should always maintain its capability of performing fast charge and discharge.

From the above discussion, it can be seen that the complex configuration and behavior of multi-source HESs present challenges to their energy management. For a balanced tradeoff among the different preferences, it is especially important to represent and take advantage of the characteristics of each device and the interactive relationship among them. In a so-called multi-agent system (MAS), a system comprising multiple agents, there are only local goals, i.e., preferences here, of each individual agent, namely no overall system goal [13]. This aspect is essentially different from the conventional centralized approaches, and well matches the aforementioned requirement from the energy management of the multi-source HESs such as the engine-generator/battery/UC HES [14]. So far in the field of power engineering the MAS-based approaches have been investigated for the applications in smart grid, microgrid, building energy system, etc [15]–[17]. For the MASs, they naturally require a decentralized decision-making method or control strategy. It is well-known that game theory is a powerful tool for representing interactions among self-interested players/agents and predicting their choices of strategies. In game theory there are several types of equilibriums, i.e., solutions, such as Nash equilibrium, Stackelberg equilibrium, and Bayesian equilibrium [18], [19]. In the present energy management problem each device is equally treated. There is no leader-follower relationship among the devices/players in the example engine-generator/battery/UC HES. The Stackelberg equilibrium is not suitable. And since the required information of each player is available in the problem, the Bayesian equilibrium is not applicable too. Thus in this paper the Nash equilibrium is used. It is the most widely used equilibrium for non-cooperative games involving two or more players [20]. A Nash equilibrium is achieved in the case that each player has chosen a strategy and no player can benefit by changing strategies unilaterally while the other players keep theirs unchanged. The relevant applications of the Nash equilibrium are now mostly in the demand-side management of the smart grid [21], [22].

This paper proposes the multi-agent modeling and game theory-based control strategy for the energy management of the engine-generator/battery/UC HES. In the approach the three devices, the engine-generator unit, battery and UC packs, are modeled and controlled as independent but related agents, namely full respect for the performance and requirements of the individual devices [23]. The non-collaborative game among the three agents/devices then settles at a Nash equilibrium, i.e., a compromised load distribution that balances the different preferences of the engine-generator unit, battery and UC packs. As discussed in the literature, compared to the centralized control approaches, this agent-based decentralized control is expected to potentially improve the synergy, and thus, the flexibility, scalability, fault-tolerance, and reliability of the HESs, and also can reduce computational complexity [13], [24]. These advanced aspects need to be explored in future research such as through quantitative comparisons with the existing approaches. To the knowledge of the authors, this paper represents one of the first attempts to develop and implement the game theory-based control for the energy management of multi-source HESs. Due to the decentralized nature of the control, it could serve as a general solution and be extended to manage complex HESs with more devices involved.

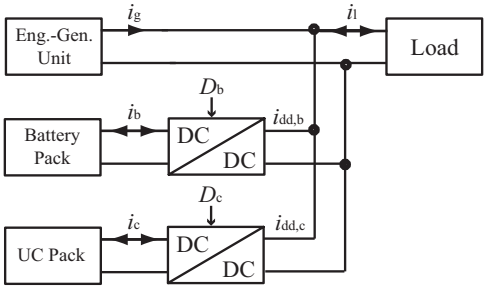

Fig. 1. The configuration of the engine-generator/battery/ultracapacitor HES.

II. Multi-agent based Modeling

A. System Configuration

The engine-generator/battery/UC HES in this paper employs the parallel-active topology, i.e., connecting DC-DC converters to the each device [see Fig. 1]. As to the engine-generator unit, it usually consists of an engine, a three-phase AC generator, a rectifier for AC-DC conversion, and a DC-DC converter

to control the output current, i_g, in Fig. 1 [6]. The HES uses two bi-directional DC-DC converters for the battery and UC packs and one uni-directional DC-DC converter that is integrated with the engine-generator unit. There are alternative topologies for the connection of the battery and UC packs such as battery semi-active and UC semi-active ones using a single DC-DC converter. In the battery semi-active hybrid the DC-DC converter connects the battery pack and the load, while in the UC semi-active hybrid the DC-DC converter is placed between the UC pack and the load. Each topology has its own advantages and disadvantages, as explained in [25]. Among these topologies, the adopted parallel-active topology is an optimal active hybrid that provides control flexibility because the devices are all controllable through the DC-DC converters. Thus it avoids UC voltage variations and enables nearly constant currents from the engine-generator unit and the battery pack. Although this topology requires three DC-DC converters, none of them needs to be full-rating.

B. Simulation Environment

A multi-agent-based modeling and programming environment, Netlogo, is used to represent the different characteristics of the three devices (engine-generator unit, battery and UC packs) and their interaction in the HES. NetLogo is an open-source software that has been widely used for modeling complex systems evolving over time [26]. It is the basic simulation environment in this paper [refer to section V]. Following the definition of MAS, in NetLogo the engine-generator unit, battery and UC packs are modeled as three agents interacting within an environment (i.e., the load demand here), as shown in Fig. 2. In this MAS each agent is independent with a different goal or preference. The utility function here is used to quantify the level of satisfaction of an agent according to the interaction between its physical model and the load demand. The purpose of the game theory-based control developed in the following sections is to find out a rule of load current distribution among the three agents. This rule should lead to a compromised solution and thus balances the different preferences of the agents.

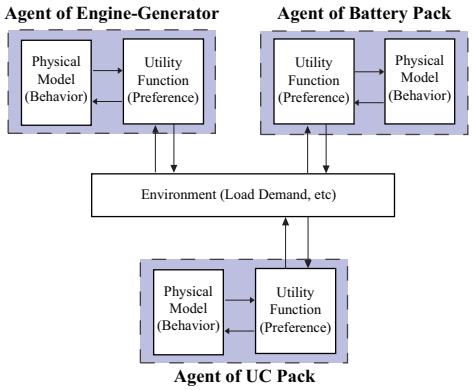

Fig. 2. The multi-agent-based modeling in Netlogo.

C. Models of Devices

In NetLogo the engine-generator unit is modeled based on the engine torque-speed map and generator efficiency map for a series HEV provided by AVL Cruise, a popular simulation tool for vehicle driveline system analysis [see Fig. 3] [27]. For the engine, its optimal torque–speed combinations under various power levels are jointly determined by using the two maps in Fig. 3(a) and (b) [8]. These combinations maximize the efficiency of the unit. As shown in Fig. 1, the power output of an engine is

$$P_e = \tau_e \omega_e, \tag{1}$$

where P_e is the engine power output; τ_e is the engine torque; and ω_e is its rotational speed. The efficiency of the generator, η_g, can be taken from the generator efficiency map in Fig. 3(b). Here the efficiency for the power conversion, η_{pc}, including the rectification and the DC-DC conversion, is assumed to be 90%. Therefore,

$$P_g = \eta_{pc} \eta_g P_e, \tag{2}$$

where P_g is the final output power from the generator-generator unit. For any specific P_g, there is only one single optimal torque-speed combination, (τ_e, ω_e). Considering a usually constant DC-link voltage, the current contributed by the engine-generator unit, i_g, is proportional to P_g. The engine-generator unit model described above is commonly used in the study of series HEVs [28]. Note the parameters of the engine-generator unit in Table I are scaled down later to match the power capability of the experimental HES discussed in section VI.

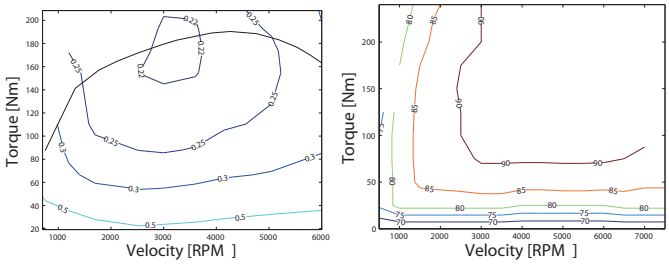

(a) (b)

Fig. 3. (a) Engine torque-speed map. (b) Generator efficiency map.

As shown in Fig. 4(a), the battery pack is modeled using its open circuit voltage (OCV), internal resistance R_b, and two resistance-capacitance (RC) networks that describe the transient response of the battery pack in second and minute ranges, i.e., $\tau_s = R_{t,s}C_{t,s}$ and $\tau_m = R_{t,m}C_{t,m}$, respectively. OCV and R_b in the battery model are obtained by using a fast averaging method, and represented by two six-ordered polynomial functions through curve fitting [29],

$$OCV = a_{ocv,0} + a_{ocv,1}x + ... + a_{ocv,6}x^6, \tag{3}$$

$$R_b = a_{r,0} + a_{r,1}x + ... + a_{r,6}x^6, \tag{4}$$

respectively, where x means SOC of the battery pack. For the model of the UC pack in Fig. 4(b), C is its capacitance; $R_{c,s}$ is the internal resistance, and $R_{c,l}$ models the leak current [30]. A pulsed current test is used to obtain the parameters of the UC pack [31]. Table I lists the measured parameters of the battery and UC cells in the final experiments.

As mentioned above, in the engine-generator/battery/UC HES, besides the uni-directional DC-DC converter integrated

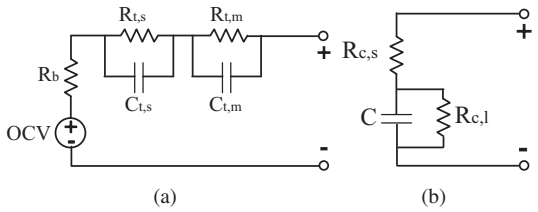

Fig. 4. Models of the devices. (a) battery pack. (b) UC pack.

TABLE I
PARAMETERS OF CELLS AND ENG.-GEN. UNIT.

Li-ion Bat. Cell			
$a_{ocv,0}$	2.30	$a_{ocv,1}$	15.96
$a_{ocv,2}$	-99.35	$a_{ocv,3}$	295.20
$a_{ocv,4}$	-446.49	$a_{ocv,5}$	331.41
$a_{ocv,6}$	-95.56	$a_{r,0}$	0.02
$a_{r,1}$	-0.24	$a_{r,2}$	1.69
$a_{r,3}$	-5.66	$a_{r,4}$	9.67
$a_{r,5}$	-8.13	$a_{r,6}$	2.67
$R_{t,s}$	5.60 mΩ	$C_{t,s}$	12.20 kF
$R_{t,m}$	2.87 mΩ	$C_{t,m}$	453.11 kF
I_{bmax}	10 A		
UC Cell			
C	1.76 kF	$R_{c,s}$	2.50 mΩ
$R_{c,l}$	3 kΩ	$I_{c,max}$	20 A
Engine			
max τ_e	190.4 Nm	max ω_e	6000 r/min
optimal τ_e	174.2 Nm	optimal ω_e	3000 r/min

within the engine-generator unit, there are two additional bi-directional buck-boost DC-DC converters. The DC-DC converter connecting the UC pack operates in voltage control mode in order to maintain a constant DC-link voltage, while the purpose of another DC-DC converter is to perform the control of the battery current, i.e., in current control mode. Detailed explanations on the DC-DC converters can be found in section VI discussing final experiments. The purpose of the simulation in section V is to verify the proposed game theory-based approach for the energy management of the multi-source HES. Thus in the simulation the dynamics of the two bi-directional DC-DC converters is simplified using the average efficiency, 98.03%, of the two real DC-DC converters in the final experiments.

III. REPRESENTATION OF PREFERENCES

Here the preferences of the three agents, the engine-generator unit, the battery and UC packs, are quantified by their respective utility functions that define the benefit to a specific agent, i.e., the satisfaction level, if it provides certain current at a particular time [32]. As mentioned above, the respective preferences of the engine-generator unit, the battery and UC packs, are 1) to supply an optimal current that maximizes the fuel economy of the engine; 2) to minimize the amplitude and variation of the battery current in order to extend the battery cycle life; 3) to minimize the difference between the present UC energy level and the desired initial level, and thus maintain the charge/discharge capability of the UC pack. The following quadratic utility functions are defined that reach their maximum values when the preferences are best met [23], [32].

A. Engine-generator Unit

The utility function of the engine-generator unit, u_g, should be defined to emphasize its fuel economy, i.e., providing a current as close as possible to the optimal current that maximizes the fuel economy. Here u_g is defined as

$$u_g = 1 - a(i_g - I_{g,opt})^2, \tag{5}$$

where i_g is the current supplied by the engine-generator unit; $I_{g,opt}$ is the optimal current. The coefficient a is designed to normalize the utility function within zero to one,

$$a = Min\left[\frac{1}{(I_{g,max} - I_{g,opt})^2}, \frac{1}{(0 - I_{g,opt})^2}\right]. \tag{6}$$

$I_{g,max}$ is the maximum permissible current from the engine-generator unit. u_g is one when i_g equals $I_{g,opt}$, while it becomes zero when i_g reaches its limits, i.e., 0 (idle state of engine) or $I_{g,max}$.

B. Battery Pack

The preference of the battery pack is to protect itself, i.e., the extension of its own cycle life. This preference relates to the amplitude and the variation rate of the battery current [3]. Thus the utility function of the battery pack, u_b, is defined as a weighted sum,

$$u_b = w_{b,ave}u_{b,ave} + w_{b,dif}u_{b,dif}, \tag{7}$$

where $w_{b,ave}$ and $w_{b,dif}$ are the weight coefficients. $u_{b,ave}$ and $u_{b,dif}$ are designed to minimize the amplitude and the variation rate of the battery current, respectively,

$$u_{b,ave} = 1 - b(i_b - i_{b,ave})^2, \tag{8}$$
$$u_{b,dif} = 1 - c(i_b - i_{b,l})^2. \tag{9}$$

Here i_b is the battery current; $i_{b,ave}$ is the average battery current so far; $i_{b,l}$ is the battery current at the last control instant. Note the variation rate of i_b is $\frac{i_b - i_{b,l}}{\Delta t}$, where Δt is the sampling period for the control. The two coefficients, b and c, are

$$b = Min\left[\frac{1}{(I_{b,max} - i_{b,ave})^2}, \frac{1}{(-I_{b,max} - i_{b,ave})^2}\right], \tag{10}$$
$$c = Min\left[\frac{1}{(I_{b,max} - i_{b,l})^2}, \frac{1}{(-I_{b,max} - i_{b,l})^2}\right], \tag{11}$$

respectively. Again the two coefficients are introduced to normalize the values of $u_{b,ave}$ and $u_{b,dif}$ between zero and one.

C. Ultracapacitor Pack

In the HES the UC pack mainly serves as an "energy buffer" that improves the performance of the overall HES, especially its responsiveness and energy efficiency. For a capacitor, the stored energy is determined by its voltage, v_c,

$$e_c = \frac{1}{2}Cv_c^2, \tag{12}$$

where C is the capacitance. Considering the equal possibilities of charge and discharge in a dynamic environment, the desired initial voltage of the UC pack, $V_{c,ini}$, can be designed as

$$V_{c,ini} = \sqrt{\frac{{V_{c,max}}^2 + {V_{c,emp}}^2}{2}}, \tag{13}$$

where $V_{c,max}$ and $V_{c,emp}$ are the maximum and minimum permissible voltages of the UC pack, respectively. At this voltage, the UC pack is half charged, and thus always ready to quickly supply or adsorb the dynamic current.

The utility function of the UC pack, u_c, can then be expressed as the closeness to the desired initial voltage, $V_{c,ini}$ in (13),

$$u_c = 1 - d(i_c - i_{c,fit})^2, \tag{14}$$

where i_c is the UC current. A positive i_c means discharge, and vice versa. $i_{c,fit}$ is the UC current under which the energy left in the UC pack will become closer to its desired initial state [refer to (13)],

$$i_{c,fit} = \left(2\frac{v_c^2 - V_{c,emp}^2}{V_{c,max}^2 - V_{c,emp}^2} - 1\right) I_{c,max}, \tag{15}$$

where $I_{c,max}$ is the maximum permissible magnitude of the charge and discharge currents of the UC pack. As shown in (15), $i_{c,fit}$ is designed to be linearly proportional to the rest energy stored in the UC pack. If the UC pack is empty or full, $i_{c,fit}$ will be the upper/lower limit current to discharge/charge the UC pack. If the energy contained in the UC pack is exactly at its middle level, $i_{c,fit}$ will be zero. Similarly the coefficient d is introduced to normalize u_c to be within zero to one,

$$d = Min\left[\frac{1}{(I_{c,max} - i_{c,fit})^2}, \frac{1}{(-I_{c,max} - i_{c,fit})^2}\right]. \tag{16}$$

D. Modification of Preferences

It is interesting to note that the degrees of freedom in the engine-generator/battery/UC HES are actually not three, but two because the UC pack is only an assistive energy storage device. The UC pack is required to work with both the engine-generator unit and the battery pack in order to meet the final load demand and improve the performance of the overall HES. Therefore, the utility functions of the engine-generator unit and the battery pack are modified as follows by combining with the utility function of the UC pack, i.e., adding the preference of the UC pack into the two utility functions [refer to (14)],

$$\begin{aligned} u_{g,c} &= w_{g,fuel}[1 - a(i_g - I_{g,opt})^2] \\ &+ w_{c,eng}[1 - d(i_c - i_{c,fit})^2], \end{aligned} \tag{17}$$

and

$$\begin{aligned} u_{b,c} &= w_{b,ave}[1 - b(i_b - i_{b,ave})^2] \\ &+ w_{b,dif}[1 - c(i_b - i_{b,l})^2] \\ &+ w_{c,eng}^{'}[1 - d(i_c - i_{c,fit})^2]. \end{aligned} \tag{18}$$

$u_{g,c}$ and $u_{b,c}$ are the modified utility functions for the engine-generator unit and the battery pack, respectively. $w_{g,fuel}$, $w_{c,eng}$, and $w_{c,eng}^{'}$ are the newly added weight coefficients. The determination of all the weight coefficients is discussed in section IV-B.

Here i_g and i_b are the two independent control variables. Then i_c can be determined as

$$i_c = \frac{i_l - i_g - (1 - D_b)i_b}{1 - D_c}, \tag{19}$$

where i_l is the final load current; D_b and D_c are the duty cycles of the two bidirectional DC-DC converters connected to the battery and UC packs, respectively.

IV. Non-cooperative Current Control Game

The different preferences of the three devices/agents, i.e., the engine-generator unit, the battery and UC packs, in the HES can be summarized as follows,

- Engine-generator unit: lower the fuel consumption;
- Battery pack: extend the cycle life;
- UC pack: maintain the charge/discharge capability.

This energy management problem can be configured as a non-cooperative current control (NCC) game, i.e., $G = [2, (i_g, i_b), (u_{g,c}, u_{b,c})]$ [18]. In this NCC game, each player (i.e., the engine-generator unit or the battery pack here) tends to maximize its own utility. However, the current that optimizes the utility function of one player depends on the current selected by another player. The two players need to negotiate and determine a set of currents that satisfies both utility functions. This operating point is the so-called "Nash equilibrium".

A. Nash Equilibrium

As mentioned in the introduction section, in the NCC game when the engine-generator unit and the battery pack achieve the Nash equilibrium, their utility functions can not both become larger if only one of the devices changes its output current. Thus the Nash equilibrium is the crossing point of two best response functions of i_g and i_b, BR_g and BR_b, defined as

$$BR_g : \frac{\partial u_{g,c}}{\partial i_g} = 0 \text{ and } BR_b : \frac{\partial u_{b,c}}{\partial i_b} = 0. \tag{20}$$

Here the best response refers to the current that maximizes the utility function of one player taking another player's current as given. The two best response functions can be rewritten as

$$i_g = \frac{w_{g,fuel}I_{g,opt}a + \frac{w_{c,eng}}{1-D_c}\left[\frac{i_l - (1-D_b)i_b}{1-D_c} - i_{c,fit}\right]d}{w_{g,fuel}a + \frac{w_{c,eng}}{(1-D_c)^2}d}, \tag{21}$$

and

$$i_b = \frac{i_{b,ave}w_{b,ave}c + i_{b,l}w_{b,dif}c - w_{c,eng}^{'}\frac{1-D_b}{1-D_c}\left(\frac{i_g - i_l}{1-D_c} + i_{c,fit}\right)d}{w_{b,ave}b + w_{b,dif}c + w_{c,eng}^{'}\frac{(1-D_b)^2}{(1-D_c)^2}d}. \tag{22}$$

Using (21)(22), the Nash equilibrium can then be reached through an iterative process from initial conditions such as $i_g = I_{g,opt}$ and $i_b = 0$ in this paper. This process is classical in game theory to locate the Nash equilibrium [20].

The two currents, i_g and i_b, at the Nash equilibrium provide a solution that balances the different preferences of the two players in the NCC game. Unlike the conventional multiobjective optimization such as using weight-sum method,

the objectives of the two players, i.e., the two utility functions $u_{g,c}$ and $u_{b,c}$, are independently maximized based on their respective local information [20], [23]. For example, i_g in (21) is determined by $u_{g,c}$'s own parameters taking i_b, another player's current, as given. The dependence on only local information makes the game theory-based control flexible to deal with complex HESs. In addition, due to the linearity of the two response functions, the solution of the NCC game is fast enough to be implemented in real time [refer to the following experimental implementation in section VI].

In order to prove the existence and uniqueness of the Nash equilibrium, (21)(22) are further written as

$$i_g = k_1 - k_2 i_b, \tag{23}$$

$$i_b = k_3 - k_4 i_g. \tag{24}$$

Thus the Nash equilibrium can be mathematically calculated as follows,

$$i_g = \frac{k_1 - k_2 k_3}{1 - k_2 k_4}, \tag{25}$$

$$i_b = \frac{k_3 - k_1 k_4}{1 - k_2 k_4}, \tag{26}$$

where from (21)(22) k_1, k_2, k_3, and k_4 are

$$k_1 = \frac{w_{g,fuel} I_{g,opt} a + \frac{w_{c,eng}}{1-D_c}\left(\frac{i_l}{1-D_c} - i_{c,fit}\right) d}{w_{g,fuel} a + \frac{w_{c,eng}}{(1-D_c)^2} d}, \tag{27}$$

$$k_2 = \frac{\frac{w_{c,eng}(1-D_b)}{(1-D_c)^2} d}{w_{g,fuel} a + \frac{w_{c,eng}}{(1-D_c)^2} d}, \tag{28}$$

$$k_3 = \frac{w_{b,ave} i_{b,ave} b + w_{b,dif} i_{b,l} c + w_{c,eng}^{'} \frac{1-D_b}{1-D_c}\left(\frac{i_l}{1-D_c} - i_{c,fit}\right) d}{w_{b,ave} b + w_{b,dif} c + w_{c,eng}^{'} \frac{(1-D_b)^2}{(1-D_c)^2} d}, \tag{29}$$

$$k_4 = \frac{w_{c,eng}^{'} \frac{1-D_b}{(1-D_c)^2} d}{w_{b,ave} b + w_{b,dif} c + w_{c,eng}^{'} \frac{(1-D_b)^2}{(1-D_c)^2} d}. \tag{30}$$

Note the Nash equilibrium always exists in this game [18]. This is because that the modified utility functions of the engine-generator unit and the battery pack are both quadratic functions, namely continuous and concave functions [refer to (17)(18)].

The above discussion actually generalizes the case of the ALD-based control. In this ideal control, the capacitance of the UC pack is assumed to be infinite. Thus it is possible to maintain a constant v_c that corresponds to the half of the total usable energy in the UC pack, namely a maximized utility of the UC pack [refer to (13)]. Then the modified utility functions, $u_{g,c}$ and $u_{b,c}$, are now equivalent to the utilities of the engine-generator unit and the battery pack themselves, respectively. Again the condition of the maximized utilities for the two players/devices is to supply constant currents, i.e., $I_{g,opt}$ for the engine generator and $I_{b,ave}$ for the battery pack. Here $I_{b,ave}$ is defined as

$$I_{b,ave} = \frac{\sum i_b}{N}, \tag{31}$$

in which an entire load profile is assumed to be preknown. N is the total number of the control instants. Only under the ideal ALD-based control all the three utilities can be maximized at the same time, and the Nash Equilibrium simply locates at $(I_{g,opt}, I_{b,ave})$.

B. Determination of Weight Coefficients

As shown in (17)(18), the solution at the Nash equilibrium can be calculated as long as the values of the weight coefficients are determined. First the sums of the weight coefficients in the two utility functions are both equal to one, namely

$$w_{g,fuel} + w_{c,eng} = 1, \tag{32}$$

$$w_{b,ave} + w_{b,dif} + w_{c,eng}^{'} = 1. \tag{33}$$

Since the UC pack is an assistive device, its weights, $w_{c,eng}$ and $w_{c,eng}^{'}$, can be calculated in an adaptive manner:

$$w_{c,eng} = w_{c,min} + \frac{1 - w_{c,min}}{V_{c,ini}^2 - V_{c,emp}^2}\left|V_{c,ini}^2 - v_c^2\right|, \tag{34}$$

$$w_{c,eng}^{'} = w_{c,min}^{'} + \frac{1 - w_{c,min}^{'}}{V_{c,ini}^2 - V_{c,emp}^2}\left|V_{c,ini}^2 - v_c^2\right|. \tag{35}$$

In (34) $w_{c,eng}$ is designed to be equal to $w_{c,min}$ when the energy (i.e., the voltage v_c) left in UC pack is in its initial state, and it becomes one when the UC pack is full or empty. $w_{c,eng}^{'}$ is determined in the same way.

The determination of $w_{c,min}$, $w_{c,min}^{'}$, $w_{b,ave}$, and $w_{b,dif}$ can be based on a target cycle such as the well-known New European Driving Cycle (NEDC) [see Fig. 5] [33]. Note the procedure developed below itself is a general one that can be applied to any other random cycles. As shown in the utility function of the battery pack, (7), $w_{b,ave}$ focuses on the long-term behavior of the battery current, while $w_{b,dif}$ emphasizes the short-term one. Meanwhile, $w_{c,min}$ and $w_{c,min}^{'}$ determine the range of the usable energy of the UC pack. They define the strength of the tendency that the UC pack reaches its desired initial voltage, $V_{c,ini}$. Various combinations of $w_{b,ave}/w_{b,dif}$, $w_{c,min}$, and $w_{c,min}^{'}$ are applied to calculate 1) the root mean square (RMS) of the battery current variation, an indication of battery cycle life [2], [3],

$$I_{b,var} = \sqrt{\frac{\sum (i_b - I_{b,l})^2}{N}}, \tag{36}$$

2) the range of usable UC energy, 3) and the fuel efficiency of the engine-generator unit.

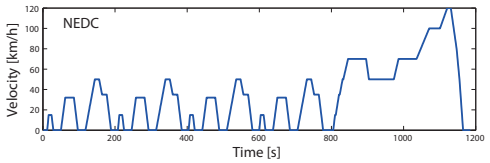

Fig. 5. Velocity profile of NEDC cycle.

The trade-off relationship among the four weights can then be represented using the Pareto set, as shown in Fig. 6 [34]. In the figure, the x, y, and z axes are the normalized ranges of usable UC energy, $I_{b,var}$, and the fuel efficiency of the engine-generator unit, respectively. In the normalization, "0" corresponds to the minimum of a variable, and "1" is the maximum. In Fig. 6 the knee point is the closest point to

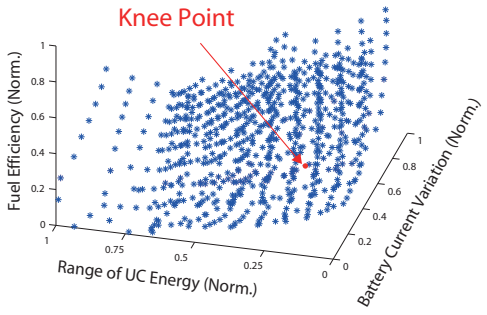

Fig. 6. Pareto set for NEDC cycle.

the origin (0,0,0). Any deviation from this point will favor one or two of the three criteria (fuel economy, protection of battery, and proper use of the UC pack), but sacrifices the other more. The knee point gives the most satisfactory solution that corresponds to the following combination of the weights under the NEDC cycle,

$$\frac{w_{b,ave}}{w_{b,dif}} = 0.3,\ w_{c,min} = 0.1,\ w^{'}_{c,min} = 0.1. \qquad (37)$$

All the other weights can then be determined accordingly using (32)–(35). Note this result and the following simulation are both based on the parameters of the final experimental HES in section VI. The NEDC cycle here is an example to develop and explain a possible solution that could serve as a starting point in real applications. As a part of future effort, an adaptive mechanism could be added to automatically tune the weight coefficients such as through the rule-based approaches [35].

V. Simulation

For validation purposes additional two other well-known cycles are also included in simulation, UDDS (Urban Dynamometer Driving Schedule) and JC08 (the Japanese urban cycle) driving cycles, as shown in Fig. 7 [33]. The weight coefficients for the three cycles (NEDC, UDDS, and JC08) are all determined by the locations of their respective knee points, and listed in Table II. In the simulation each cycle runs four times continuously in order to represent a long-term (≈1.3 hours) and dynamic load demand. In order to present full-scale power, the simulated power level is 100 times greater than that of the final experimental HES.

TABLE II
Weight Coefficients for Cycles.

Weight Coefficients	NEDC	UDDS	JC08
$\frac{w_{b,ave}}{w_{b,dif}}$	0.3	0.2	0.1
$w_{c,min}$	0.1	0.2	0.2
$w^{'}_{c,min}$	0.1	0.2	0.8

A. Sizing of Devices

Proper sizing is very important when designing a HES. Comprehensive discussions on the sizing issue can be found in [36], [37]. The sizing discussed below only serves as an example to facilitate the validation of the proposed approach. As shown in Figs. 5, 7, and 8, among the three cycles the longest and fastest acceleration occurs in the NEDC cycle

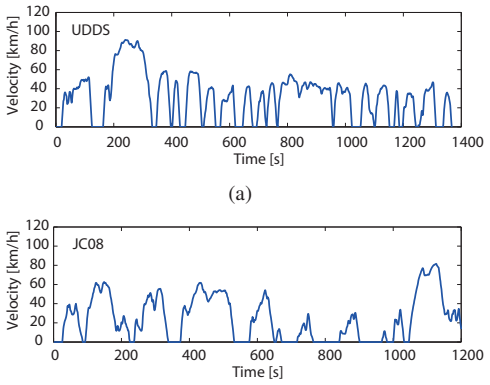

Fig. 7. Velocity profiles of the two additional cycles. (a) UDDS cycle. (b) JC08 cycle.

between 904 s and 1130 s, which makes the NEDC cycle the most challenging. Thus the size of the battery pack here is designed to provide one third of the average power in the NEDC cycle, and the engine-generator unit will supply the rest two thirds working at its maximum efficiency point. In order to supply the dynamic load current within 904 s to 1130 s, the required total energy is 3.36 MJ. Because the UC pack is an "energy buffer", it is desirable that this amount of energy can be provided by the UC pack using the half of its total capacitance [refer to section III-C]. The above sizing also makes it possible to compare with the performance of the ALD-based control, in which the UC pack is required to provide the entire dynamic load current. Note ALD-based control here is a quasi-ideal one because the capacitance of UC pack is sufficiently large, but is not infinite.

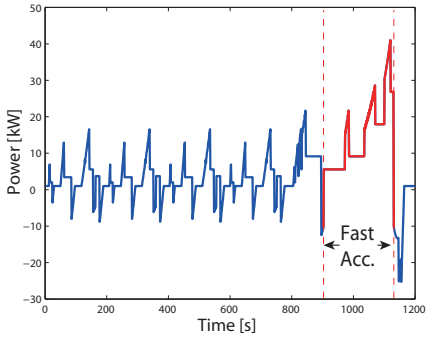

Fig. 8. Power profile of NEDC cycle.

B. Quantitative Criteria

As discussed in section IV-B, the average fuel consumption of the engine-generator unit ($C_{g,ave}$), the average battery current ($I_{b,ave}$), the RMS of the battery current variation ($I_{b,var}$), and the average energy contained in the UC pack ($E_{c,ave}$) are selected as four quantitative criteria [refer to (31)(36)(38)(39)]. They are used to compare the performances of the game theory-based, the ALD-based control, and the power-flow

control under the three cycles.

$$C_{g,ave} = \frac{\sum C_g}{N}, \quad (38)$$

$$E_{c,ave} = \frac{\sum C(v_c^2 - V_{c,emp}^2)}{2N}, \quad (39)$$

where C_g is the sampled instantaneous fuel efficiency of the engine-generator unit.

C. Comparisons and Results

Here the results of the ideal ALD-based control and the power-flow control are used for comparison purposes [4], [9].

- ALD-based control: the engine-generator unit works at its maximum efficiency point (i.e., a constant i_g=$I_{g,opt}$), and the battery pack supplies the rest of the required average current, while the UC pack covers the entire dynamic load current. Note here the ALD-based control mainly serves as an ideal case for reference purposes, in which the entire future load demand is assumed to be exactly pre-known. This assumption is usually impractical in real applications.
- Power-flow control: This alternative approach was proposed in [4], a well-cited one among few existing references discussing the control of an engine-generator/battery/UC HES. In the reference the so-called "power assistance mode" simultaneously uses the three devices, in which engine is at idle state during deceleration. Engine also needs to charge the UC pack when the UC voltage is lower than a desired value, $V_{c,ini}$ in (13) here. For comparison purposes, again the battery pack is assumed to provide the one third of the average power in the cycles to assist the engine during acceleration. As same as in [4], the engine-generator unit supplies power within its limitation and charges the UC pack when needed, while the UC pack covers the rest of the required power.

Table III summarizes the results of the game theory(GT)-based control, the ALD-based control, and the power-flow control. In all the three cycles, NEDC, UDDS, and JC08 cycles, the game theory-based control achieves a comparable performance to that of the ideal ALD-basd control. This result shows that in the game theory-based control the different preferences of the three devices are well met simultaneously. Meanwhile, the game theory-based control is a more practical solution that does not require exact information of the entire cycles. Besides, the game theory-based control outpaces the power-flow control in terms of both fuel economy and protection of battery, i.e., much smaller $I_{b,var}$. For the ALD- and game theory-based control, the difference in $E_{c,ave}$ is relatively large under the NEDC cycle due to the long-period strong acceleration in the cycle, especially within 904–1130 s. Unlike the ideal ALD-based control, the game theory-based control does not require the exact preknowledge of the cycles in advance. Naturally under the most challenging NEDC cycle its control performance deteriorates compared to the performance of the ALD-based control. Due to the similar reason, in the NEDC cycle the difference in $E_{c,ave}$ between the ALD-based control and power-flow control is even larger.

TABLE III
COMPARISON ON VALUES OF CRITERIA.

Control Method	$C_{g,ave}$ (L/kWh)	$I_{b,ave}$ (A)	$I_{b,var}$ (A)	$E_{c,ave}$ (MJ)
[NEDC]:				
GT-based	0.2431	5.43	0.0048	3.70
ALD-based	0.2355	5.57	0	4.94
Power-flow	0.2536	4.31	0.1830	3.11
[UDDS]:				
GT-based	0.2382	4.01	0.0014	3.03
ALD-based	0.2355	3.82	0	3.20
Power-flow	0.2567	3.66	0.2501	3.38
[JC08]:				
GT-based	0.2356	0.90	0.0004	3.54
ALD-based	0.2355	0.45	0	3.64
Power-flow	0.2794	2.77	0.1956	3.55

It is because in the power-flow control the UC voltage is not fully controlled.

The simulated load currents from the engine-generator unit, battery and UC packs are shown in Fig. 9. Note again in the ALD-based control the losses from the bi-directional two DC-DC converters are assumed to be exactly pre-known and have to be considered in order to reach a truly optimal solution. Thus its load current from the battery pack is higher than that using the power-flow control in the NEDC cycle [see Fig. 9(a)]. Under the game theory-based control, the engine-generator unit provides an almost constant current; the UC pack covers most of the dynamic current in all the three cycles. The currents supplied by the battery pack in the UDDS and JC08 cycles are smooth; while in the NEDC cycle, the variation of the current from the battery pack is relatively large due to the strong acceleration between 904–1130 s. This result actually well demonstrates the basic consideration of the Nash Equilibrium and the game theory-based control. In the beginning of the NEDC cycle before 904 s, the required power is relatively low; therefore, the UC pack is capable to provide the entire dynamic current, i.e., keeps being discharged and charged. As shown in (34)(35), the weights of the UC pack, $w_{c,eng}$ and $w_{c,eng}^{'}$, are adaptively updated with v_c, the present voltage (i.e., SOC) of the UC pack. Closer v_c to the initial voltage, $V_{c,ini}$, smaller the two weights, $w_{c,eng}$ and $w_{c,eng}^{'}$. Thus before 904 s, the Nash Equilibrium mainly emphasizes the utilities of the engine-generator unit and the battery pack [refer to (17)(18)], and in the best response functions, BR_g and BR_b in (20), a predominant requirement is to smooth the currents from the engine-generator unit and the battery pack. However, between 904–1130 s v_c significantly deviates from $V_{c,ini}$ due to the strong acceleration, namely bigger $w_{c,eng}$ and $w_{c,eng}^{'}$ [see Fig. 10]. Thus in the NCC game the utility of the UC pack, maintaining its initial voltage, is more emphasized, and the engine-generator unit and the battery pack are also required to supply a certain part of the dynamic current. Since in the Pareto set the fuel efficiency is emphasized, the battery pack supplies more dynamic current due to its higher energy efficiency. Meanwhile, under the power-flow control the engine frequently operates at its idle state, and the current from the engine-generator unit is not continuous. This leads to discontinuous battery current, which

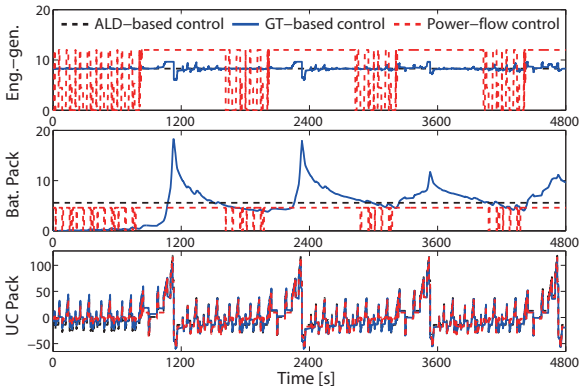

(a)

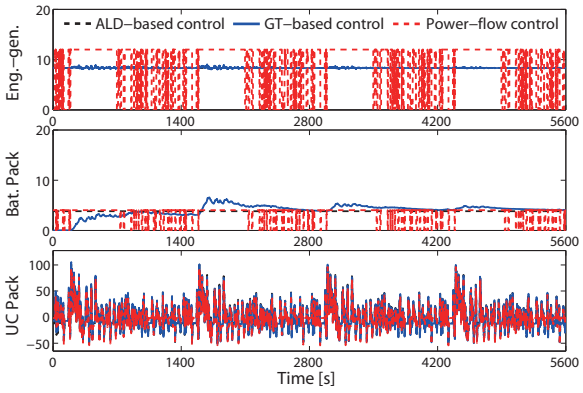

(b)

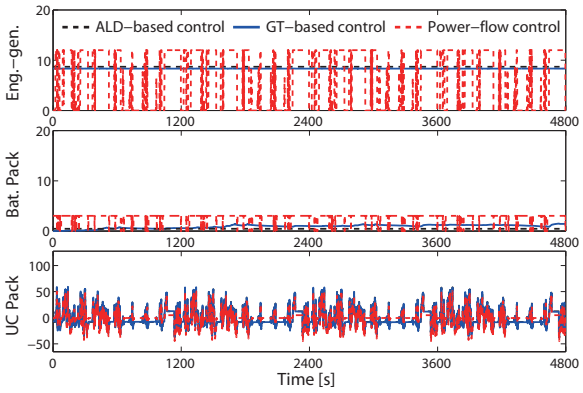

(c)

Fig. 9. The load currents (A) supplied by the engine-generator unit, battery and UC packs under GT-based control (blue solid line), ALD-based control (black dashed line), and power-flow control (red dashed line). (a) NEDC cycle. (b) UDDS cycle. (c) JC08 cycle.

may adversely influence the battery cycle life. Besides, the UC voltage is under a simple control. Thus different with the results under the ALD- and game theory-based control, the UC voltage at the end of the cycles does not converge to its initial desired voltage, especially in the NEDC cycle [see Fig. 10(a)].

Fig. 11 shows the trajectories of the Nash Equilibrium points, i.e., the combination of the engine-generator and battery currents (i_g and i_b), in the three cycles. The trajectories indicate two critical aspects of the control of the engine-generator/battery/UC HES:

1) Sizing: The range of the Nash equilibrium points relates to the sizing. In this paper the sizing of the UC pack is determined by the NEDC cycle due to its long-period strong acceleration within 904–1130 s. Thus the UC pack is relatively over-sized for the UDDS and JC08 cycles. This explains the smaller variation ranges of the Nash equilibrium points in the two cycles, namely smoother i_g and i_b. Note with an infinite large UC pack, the Nash equilibrium point will always locate in a fixed position, i.e., a control strategy taken by the ideal ALD-based control.
2) Convergence: After more repeated cycles, Nash equilibrium points become closer to the operating points of the ideal ALD-based control in all the three cycles. It means that with more history data, the results, currents and voltages, of the game theory-based control will converge to those of the ALD-based control. The current and voltage responses in Fig. 9 and Fig. 10 also indicate this trend.

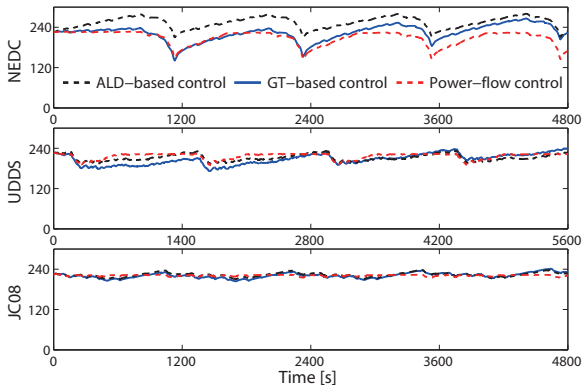

Fig. 10. The voltages (V) of the UC pack under GT-based control (blue solid line), ALD-based control (black dashed line), and power-flow control (red dashed line).

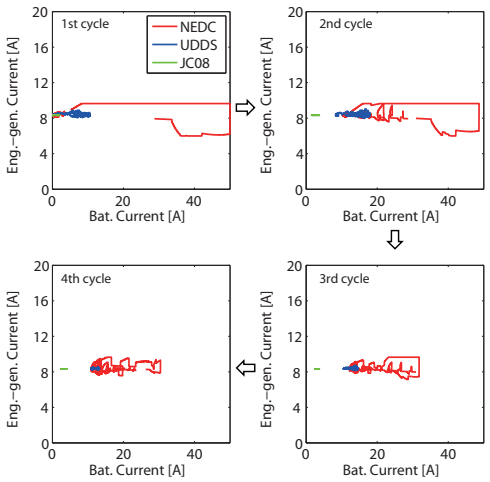

Fig. 11. The trajectories of the Nash equilibrium points.

For reference purposes, the simulated average efficiencies of the battery and UC packs, η_b, and η_c, are calculated and summarized in Table IV. Since the engine efficiency map is not available for the engine model in AVL Cruise, the engine fuel consumption in Table III is shown again that reflects the engine efficiency. As discussed above, the fuel economy of the

TABLE IV
COMPARISON ON EFFICIENCIES.

Control Method	$C_{g,ave}$ (L/kWh)	η_b (%)	η_c (%)
[NEDC]:			
GT-based	0.2431	96.58	87.51
ALD-based	0.2355	96.95	87.16
Power-flow	0.2536	97.13	86.12
[UDDS]:			
GT-based	0.2382	97.18	89.42
ALD-based	0.2355	97.27	89.43
Power-flow	0.2567	97.23	89.14
[JC08]:			
GT-based	0.2356	97.80	92.64
ALD-based	0.2355	97.91	92.64
Power-flow	0.2794	97.42	91.89

TABLE V
SPECIFICATIONS FOR MAJOR COMPONENTS.

Li-ion Battery Pack (Lishen LP2770102AC)	Two cells (Series), 12.5 Ah/cell, 3.2 V/cell (Nominal Vol.)
UC Pack (Nippon Chemi-Con DLE series)	Twelve cells (6 Series 2 Parallel) 1760 F/cell, 2.5 V/cell (Max Vol.)
DC-DC Converter (100 W) (Design/fabricate in house)	Switch Frequency: 20kHz L: 500 μH, C: 2 mF R_{S1}, R_{S2}: 12 mΩ
DC-DC Converter (400 W) (Design/fabricate in house)	Switch Frequency: 20kHz L: 200 μH, C: 2 mF R_{S1}, R_{S2}: 7.5 mΩ
Electronic Load (Kikusui PLZ-50F/150U)	Max Power: 600W (1 PLZ-50F, 4 PLZ150Us with 1.5–150V 0–30A each)
Power Supply (Takasago ZX-800L)	Max Power: 800W 0–80V, 0–80A)

game theory-based control is better than that of the power-flow control, and comparable to the fuel economy under the ideal ALD-based control. The engine-generator unit is the main energy source in the HES, and its maximum efficiency is the lowest, usually less than 30% [8]. Thus the overall efficiency of the HES basically follows the same trend as the engine fuel economy. As to the efficiencies of the battery and UC packs, η_b and η_c, again the game theory-based control shows a comparable performance to that of the ideal ALD-based control. For the power-flow control, its η_b's in the NEDC and UDDS are the highest because the battery current is zero when the engine is at the idle state, i.e., a smaller battery average current over time. Meanwhile, in the JC08 cycle the constant battery current in the power-flow control is much higher than the currents in the ALD- and game theory-based control [see Fig. 9(c)]. Thus η_b under the power-flow control is the lowest in JC08 cycle.

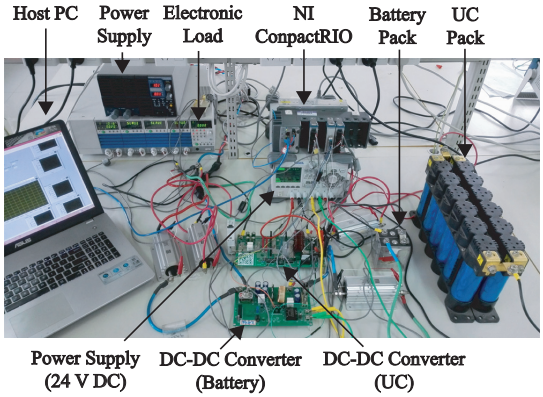

(a)

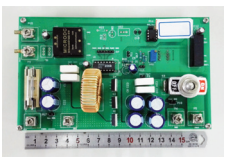

(b)

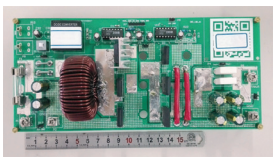

(c)

Fig. 12. Experimental parallel-active HES. (a) System. (b) The Bi-directional DC-DC converter for battery pack (peak power 100 W). (c) The Bi-directional DC-DC converter for UC pack (peak power 400 W).

VI. EXPERIMENTAL IMPLEMENTATION

As shown in Fig. 12, the three cycles are emulated through the combination of the power supply and the electronic load. The National Instrument (NI) CompactRIO system collects data, and performs the PWM (power-width-modulation) control of the two DC-DC converters following the reference commands from the host PC. In this experimental setup the engine model (i.e., the engine torque-speed map in Fig. 3(a)) is implemented in the host PC. This virtual implementation of the engine-generator unit is a common practice in existing research [38], [39]. In the experiments the parameters of the engine-generator unit, battery and UC packs, and the cycles are scaled down to match the power capability of the experimental HES. The specifications for the battery and UC packs, the DC-DC converters, the electronic load, and the power supply are listed in Table. V. The two bi-directional DC-DC converters connecting the battery and UC packs are the classical buck-boost DC-DC converters [40]. Fig. 13 shows the circuit topology, blockdiagrams for the current and voltage control of the converters. As shown in Fig. 12, the DC-DC converter with peak power 100 W is connected with the battery pack, and thus in the current control mode, while the UC pack is connected with the 400 W peak power DC-DC converter, and its output voltage is controlled, i.e., in the voltage control mode. $v_{dc-link}$ is the DC-link voltage. In the two control modes both the current and voltage controllers are PI (Proportional-Integral) controllers implemented using the NI CompactRIO system.

The Nash equilibrium of the engine-generator and battery currents, i_g and i_b, in (25)(26) is updated in the host PC at every control instant with an interval of 0.1 s. In the LabVIEW program each player of the NCC game (i.e., the engine-generator unit and the battery) owns its independent while loop. Those two while loops are run based on their respective utility functions, local information of the individual players, and the output current of another player. The load current supplied from the UC pack is then determined accordingly. The blockdiagram for the implementation of the game theory-based control is shown in Fig. 14. The input/output data flow and the algorithm exactly follow (21)(22), through which the Nash equilibrium is iteratively calculated.

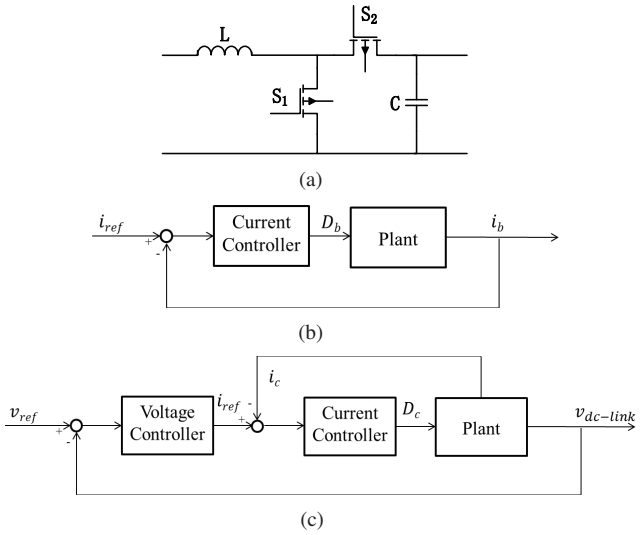

Fig. 13. Bi-directional DC-DC converters. (a) Circuit topology. (b) Blockdiagram for battery current control. (c) Blockdiagram for UC voltage control.

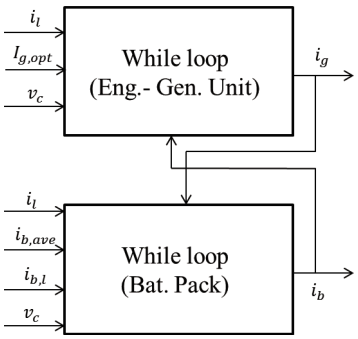

Fig. 14. Game theory-based controller.

Experiments were conducted under all the three cycles. For the sake of simplicity, here only the experimental results under the NEDC cycle, the most challenging one, are shown here in Fig. 15. The currents and voltages are collected using NI 9219 module, a universal measurement device, and plotted using standard MATLAB plotting command. It can be seen that the trend of the experimental results well matches that of the simulation results in Figs. 9(a) and 10. This validates the real-time implementation of the game theory-based control and the correctness of the previous theoretical discussions. In the final experiments the load current supplied by the battery pack is larger than that in the simulation. It is because extra energy losses occur in real circuits. In order to meet the final load demand, the HES needs to provide more energy in experiments. Since the engine-generator unit is virtually implemented, most of the additional energy is supplied by the battery pack. Again in the experiments a clear trend of convergence can be observed.

The values of the four criteria, fuel consumption, average battery current, the RMS of the battery current variation, and the average UC energy, in experiments are listed and compared in Table VI. Efficiencies of the battery and UC packs are also added in Table VII. These quantitative results are similar to those in the simulation. Due to the noise and sampling error,

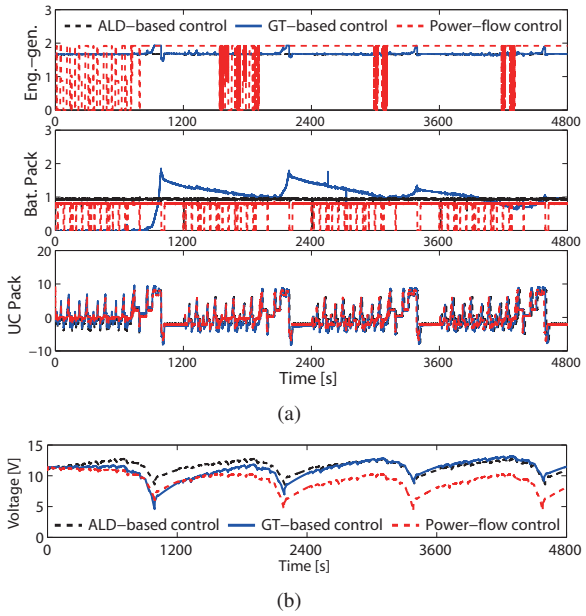

Fig. 15. Experimental current (A) and voltage (V) responses under NEDC cycle. (a) The load currents supplied by the engine-generator unit, battery and UC packs. (b) The voltage of the UC pack.

$I_{b,var}$ in the ideal ALD-based control is not zero anymore. This slightly influences the other results in the ALD-based control. Note the two DC-DC converters have an average efficiency of 98.03% in experiments. The percentages of the improvements are further shown in Table VIII by comparing the experimental results of the game theory-based control and the existing power-flow control. Besides the average fuel consumption of the engine-generator unit ($C_{g,ave}$), both the RMS of the battery current variation ($I_{b,var}$) and the average variation of UC energy from its initial level ($|\Delta E_{c,ave}|$ in (40)) are obviously decreased. Here the initial UC energy is 38.24 kJ. As discussed above, it is known that a smaller $I_{b,var}$ indicates extended battery cycle life [41]; and the decreased $|\Delta E_{c,ave}|$ shows better maintenance of UC charge/discharge capability. The improvements in Table VIII well reflect the different preferences of the three devices defined through their respective utility functions [refer to section III]. Note the improvement of the average fuel consumption, $C_{g,ave}$, in the JC08 cycle is the most obvious because in the cycle the engine most frequently operates at its idle state under the existing power-flow control [refer to Fig. 9(c)].

$$|\Delta E_{c,ave}| = \frac{\sum C|(v_c^2 - V_{c,emp}^2) - V_{c,ini}^2|}{2N} \qquad (40)$$

VII. Conclusions

This paper proposes and experimentally implements the game theory-based approach for the energy management of the multi-source engine-generator/battery/UC HES. The energy management problem is formulated as a non-cooperative current control (NCC) game. The Nash equilibrium is then analytically derived as a balanced solution that compromises the different preferences of the independent devices. Both the simulation and experimental results show the game theory-based control has a comparable performance to that of the

TABLE VI
COMPARISON ON VALUES OF CRITERIA IN EXPERIMENTS.

Control Method	$C_{g,ave}$ (L/kWh)	$I_{b,ave}$ (A)	$I_{b,var}$ (A)	$E_{c,ave}$ (kJ)
[NEDC]:				
GT-based	0.2431	0.89	0.0077	35.97
ALD-based	0.2355	0.79	0.0015	39.51
Power-flow	0.2535	0.66	0.0168	28.93
[UDDS]:				
GT-based	0.2433	0.97	0.0083	33.89
ALD-based	0.2355	0.74	0.0014	35.95
Power-flow	0.2587	0.67	0.0207	29.38
[JC08]:				
GT-based	0.2358	0.24	0.0075	37.16
ALD-based	0.2355	0.20	0.0013	36.37
Power-flow	0.2848	0.66	0.0232	35.38

TABLE VII
COMPARISON ON EFFICIENCIES IN EXPERIMENTS.

Control Method	$C_{g,ave}$ (L/kWh)	η_b (%)	η_c (%)
[NEDC]:			
GT-based	0.2431	95.64	86.18
ALD-based	0.2355	96.65	88.88
Power-flow	0.2535	96.30	83.22
[UDDS]:			
GT-based	0.2433	95.70	88.73
ALD-based	0.2355	96.51	89.76
Power-flow	0.2587	96.37	88.74
[JC08]:			
GT-based	0.2358	97.35	91.80
ALD-based	0.2355	97.76	91.60
Power-flow	0.2848	97.35	91.79

TABLE VIII
IMPROVEMENTS (%) IN EXPERIMENTS.

Cycles	$C_{g,ave}$	$I_{b,var}$	$\lvert\Delta E_{c,ave}\rvert$
NEDC	4.10% ↓	54.17% ↓	75.62% ↓
UDDS	5.95% ↓	59.90% ↓	74.15% ↓
JC08	17.21% ↓	67.67% ↓	62.24% ↓

ideal ALD-based control. This result shows that in the game theory-based control the different preferences of the devices are well met simultaneously. In addition, the game theory-based approach is a practical solution that does not require the exact future information of the entire cycles. A good convergence to the desired UC initial voltage is also shown, which is important for improving the overall performance of the HES. As summarized in Table VIII, the game theory-based control outpaces the existing power-flow control in terms of fuel consumption, protection of battery, and maintenance of UC charge/discharge capability. It is because in the game theory-based control the performance and requirements of the individual devices are fully respected. This unique advantage well matches the nature of the multi-source HES.

This paper represents an initial attempt to systematically apply the game theory-based approach in the energy management of a multi-source HES. It is important to further explore and demonstrate the advanced aspects of the game theory-based approach such as improved flexibility, scalability, and reliability of HESs. An adaptive tuning of the weight coefficients should also be discussed that enables the proposed approach to automatically fit any targeted cycle. The game theory-based approach developed in this paper will be extended to solve the energy management problem in more complicated hybrid energy systems such as a microgrid in the future.

REFERENCES

[1] J. Moreno, M. E. Ortúzar, and J. W. Dixon, "Energy-management system for a hybrid electric vehicle, using ultracapacitors and neural networks," *IEEE Trans. Ind. Electron.*, vol. 53, no. 2, pp. 614–623, 2006.

[2] S. Dusmez and A. Khaligh, "A supervisory power splitting approach for a new ultracapacitor-battery vehicle deploying two propulsion machines," *IEEE Trans. Ind. Informat.*, vol. 10, no. 3, pp. 1960–1971, 2014.

[3] J. Shen, S. Dusmez, and A. Khaligh, "Optimization of sizing and battery cycle life in battery/ultracapacitor hybrid energy storage systems for electric vehicle applications," *IEEE Trans. Ind. Informat.*, vol. 10, no. 4, pp. 2112–2121, Nov 2014.

[4] H. Yoo, S.-K. Sul, Y. Park, and J. Jeong, "System integration and power-flow management for a series hybrid electric vehicle using supercapacitors and batteries," *IEEE Trans. Ind. Appl.*, vol. 44, no. 1, pp. 108–114, 2008.

[5] Z. Amjadi and S. S. Williamson, "Power-electronics-based solutions for plug-in hybrid electric vehicle energy storage and management systems," *IEEE Trans. Ind. Electron.*, vol. 57, no. 2, pp. 608–616, 2010.

[6] K. Çağatay Bayindir, M. A. Gözüküçük, and A. Teke, "A comprehensive overview of hybrid electric vehicle: Powertrain configurations, powertrain control techniques and electronic control units," *Energy Convers. Manage.*, vol. 52, no. 2, pp. 1305–1313, 2011.

[7] S. G. Wirasingha and A. Emadi, "Classification and review of control strategies for plug-in hybrid electric vehicles," *IEEE Trans. Veh. Technol.*, vol. 60, no. 1, pp. 111–122, 2011.

[8] S. Di Cairano, W. Liang, I. V. Kolmanovsky, M. L. Kuang, and A. M. Phillips, "Power smoothing energy management and its application to a series hybrid powertrain," *IEEE Trans. Control Syst. Technol.*, vol. 21, no. 6, pp. 2091–2103, 2013.

[9] C. Zhao, H. Yin, Z. Yang, and C. Ma, "Equivalent series resistance-based energy loss analysis of a battery semiactive hybrid energy storage system," *IEEE Trans. Energy Convers.*, vol. 30, no. 3, pp. 1081–1091, Sept 2015.

[10] A. Kuperman, I. Aharon, S. Malki, and A. Kara, "Design of a semi-active battery-ultracapacitor hybrid energy source," *IEEE Trans. Power Electron.*, vol. 28, no. 2, pp. 806–815, 2013.

[11] C. G. Hochgraf, J. K. Basco, T. P. Bohn, and I. Bloom, "Effect of ultracapacitor-modified PHEV protocol on performance degradation in lithium-ion cells," *J. Power Sources*, vol. 246, pp. 965–969, 2014.

[12] P. Sharma and T. Bhatti, "A review on electrochemical double-layer capacitors," *Energy Convers. Manage.*, vol. 51, no. 12, pp. 2901–2912, 2010.

[13] S. D. McArthur, E. M. Davidson, V. M. Catterson, A. L. Dimeas, N. D. Hatziargyriou, F. Ponci, and T. Funabashi, "Multi-agent systems for power engineering applications part I: concepts, approaches, and technical challenges," *IEEE Trans. Power Syst.*, vol. 22, no. 4, pp. 1743–1752, 2007.

[14] P. Vrba, V. Marik, P. Siano, P. Leitão, G. Zhabelova, V. Vyatkin, and T. Strasser, "A review of agent and service-oriented concepts applied to intelligent energy systems," *IEEE Trans. Ind. Informat.*, vol. 10, no. 3, pp. 1890–1903, 2014.

[15] P. Zhao, S. Suryanarayanan, and M. G. Simões, "An energy management system for building structures using a multi-agent decision-making control methodology," *IEEE Trans. Ind. Appl.*, vol. 49, no. 1, pp. 322–330, 2013.

[16] E. Kremers, J. G. de Durana, and O. Barambones, "Multi-agent modeling for the simulation of a simple smart microgrid," *Energy Convers Manage*, vol. 75, pp. 643–650, 2013.

[17] C.-S. Karavas, G. Kyriakarakos, K. G. Arvanitis, and G. Papadakis, "A multi-agent decentralized energy management system based on distributed intelligence for the design and control of autonomous poly-generation microgrids," *Energy Convers Manage*, vol. 103, pp. 166–179, 2015.

[18] D. Fudenberg and J. Tirole, "Game theory," *MIT Press Books*, vol. 1, 1991.

[19] C. Dextreit and I. V. Kolmanovsky, "Game theory controller for hybrid electric vehicles," *IEEE Trans. Control Syst. Technol.*, vol. 22, no. 2, pp. 652–663, 2014.

[20] T. Basar, G. J. Olsder, G. Clsder, T. Basar, T. Baser, and G. J. Olsder, *Dynamic noncooperative game theory*. SIAM, 1995, vol. 200.

[21] I. Atzeni, L. G. Ordóñez, G. Scutari, D. P. Palomar, and J. R. Fonollosa, "Demand-side management via distributed energy generation and storage optimization," *IEEE Trans. Smart Grid*, vol. 4, no. 2, pp. 866–876, 2013.
[22] E. R. Stephens, D. B. Smith, and A. Mahanti, "Game theoretic model predictive control for distributed energy demand-side management," *IEEE Trans. Smart Grid*, vol. 6, no. 3, pp. 1394–1402, 2015.
[23] H. Yin, C. Zhao, M. Li, and C. Ma, "Utility function-based real-time control of a battery ultracapacitor hybrid energy system," *IEEE Trans. Ind. Informat.*, vol. 11, no. 1, pp. 220–231, Feb 2015.
[24] J. M. Guerrero, M. Chandorkar, T.-L. Lee, and P. C. Loh, "Advanced control architectures for intelligent microgrids, part i: decentralized and hierarchical control," *IEEE Trans. Ind. Electron.*, vol. 60, no. 4, pp. 1254–1262, 2013.
[25] A. Kuperman and I. Aharon, "Battery–ultracapacitor hybrids for pulsed current loads: A review," *Renew. Sust. Energy. Rev.*, vol. 15, no. 2, pp. 981–992, 2011.
[26] S. Tisue and U. Wilensky, "Netlogo: Design and implementation of a multi-agent modeling environment," in *Proc. of agent*, Chicago, IL, USA, Oct. 2004, pp. 7–9.
[27] AVL Cruise: https://www.avl.com/cruise.
[28] M. Gokasan, S. Bogosyan, and D. J. Goering, "Sliding mode based powertrain control for efficiency improvement in series hybrid-electric vehicles," *IEEE Power Electron. Lett.*, vol. 21, no. 3, pp. 779–790, 2006.
[29] S. Abu-Sharkh and D. Doerffel, "Rapid test and non-linear model characterisation of solid-state lithium-ion batteries," *J. Power Sources*, vol. 130, no. 1, pp. 266–274, 2004.
[30] M. S. Chan, K. Chau, and C. Chan, "Effective charging method for ultracapacitors," *Journal of Asian Electric Vehicles*, vol. 3, no. 2, pp. 771–776, 2005.
[31] W. Lajnef, J.-M. Vinassa, O. Briat, S. Azzopardi, and E. Woirgard, "Characterization methods and modelling of ultracapacitors for use as peak power sources," *J. Power Sources*, vol. 168, no. 2, pp. 553–560, 2007.
[32] R. T. Clemen and T. Reilly, *Making hard decisions with Decision Tools Suite*. Duxbury, 1999.
[33] S. Chopra and P. Bauer, "Driving range extension of EV with on-road contactless power transfer-a case study," *IEEE Trans. Ind. Electron.*, vol. 60, no. 1, pp. 329–338, 2013.
[34] J. Arora, *Introduction to optimum design*. Academic Press, 2004.
[35] W. Zhou, M. Li, H. Yin, and C. Ma, "An adaptive fuzzy logic based energy management strategy for electric vehicles," in *2014 IEEE 23rd International Symposium on Industrial Electronics (ISIE)*, Istanbul, Turkey, June 1-4, 2014, pp. 1778–1783.
[36] A. Ostadi, "Optimal sizing of battery/ultracapacitor-based energy storage systems in electric vehicles," A Ph.D. thesis presented to the University of Waterloo, Canada, 2015.
[37] A. Kuperman, M. Mellincovsky, C. Lerman, I. Aharon, N. Reichbach, G. Geula, and R. Nakash, "Supercapacitor sizing based on desired power and energy performance," *IEEE Power Electron. Lett.*, vol. 29, no. 10, pp. 5399–5405, 2014.
[38] S. G. Li, S. Sharkh, F. C. Walsh, and C.-N. Zhang, "Energy and battery management of a plug-in series hybrid electric vehicle using fuzzy logic," *IEEE Trans. Veh. Technol.*, vol. 60, no. 8, pp. 3571–3585, 2011.
[39] L. Wang, Y. Zhang, C. Yin, H. Zhang, and C. Wang, "Hardware-in-the-loop simulation for the design and verification of the control system of a series–parallel hybrid electric city-bus," *Simulation Modelling Practice and Theory*, vol. 25, pp. 148–162, 2012.
[40] M. B. Camara, H. Gualous, F. Gustin, and A. Berthon, "Design and new control of dc/dc converters to share energy between supercapacitors and batteries in hybrid vehicles," *IEEE Trans. Veh. Technol.*, vol. 57, no. 5, pp. 2721–2735, 2008.
[41] C. Zhao, H. Yin, and C. Ma, "Quantitative evaluation of lifepo4 battery cycle life improvement using ultracapacitors," *IEEE Trans. Power Electron.*, vol. 31, no. 6, pp. 3989–3993, 2015.

He Yin (S'13) received the B.S. degree in the electrical and computer engineering from the University of Michigan-Shanghai Jiao Tong University Joint Institute, Shanghai Jiao Tong University, Shanghai, China in 2012. He is currently working toward Ph.D. degree in the same institute. His research interests include optimization and decentralized control of hybrid energy systems and wireless power transfer systems.

Chen Zhao (S'14) received the B.S. degree in electrical engineering and automation from East China University of Science and Technology, Shanghai, China, in 2011. He is currently working toward Ph.D. degree in electrical and computer engineering from the University of Michigan-Shanghai Jiao Tong University Joint Institute, Shanghai Jiao Tong University, Shanghai, China. His research interests include modeling and testing of lithium-ion batteries and control of battery-ultracapacitor energy systems.

Mian Li currently is an associate professor in the University of Michigan-Shanghai Jiao Tong University Joint Institute, adjunct associate professor at the school of mechanical Engineering, at Shanghai Jiao Tong University, Shanghai, China. He received his Ph.D. degree from the Department of Mechanical Engineering, University of Maryland at College Park in December 2007 with the Best Dissertation Award. He received his BE (1994) and MS (2001) both from Tsinghua University, China. At the University of Michigan-Shanghai Jiao Tong University Joint Institute, his research work has been focused on robust/reliability based multidisciplinary design optimization and control, including topics such as multidisciplinary design optimization, robust/reliability control, sensitivity analysis, and system modeling.

Chengbin Ma (M'05) received the B.S. (Hons.) degree in industrial automation from East China University of Science and Technology, Shanghai, China, in 1997, and the M.S. and Ph.D. degrees both in the electrical engineering from University of Tokyo, Japan, in 2001 and 2004, respectively. He is currently an assistant professor of electrical and computer engineering with the University of Michigan-Shanghai Jiao Tong University Joint Institute, Shanghai Jiao Tong University, China. He is also with a joint faculty appointment in School of Mechanical Engineering, Shanghai Jiao Tong University. Between 2006 and 2008, he held a post-doctoral position with the Department of Mechanical and Aeronautical Engineering, University of California Davis, USA. From 2004 to 2006, he was a R&D researcher with Servo Laboratory, Fanuc Limited, Japan. His research interests include networked hybrid energy systems, wireless power transfer, and mechatronic control.

Mo-Yuen Chow (S'81, M'82, SM'93, F'07) earned his degree in Electrical and Computer Engineering from the University of Wisconsin-Madison (B.S., 1982); and Cornell University (M. Eng., 1983; Ph.D., 1987). Dr. Chow joined the Department of Electrical and Computer Engineering at North Carolina State University as an Assistant Professor in 1987, Associate Professor in 1993, and Professor since 1999. Dr. Chow was a Changjiang Scholar and a Qiushi Professor at Zhejiang University.

Dr. Chow's recent research focuses on distributed control, and fault management on smart grids, batteries, and robotic systems. Dr. Chow has established the Advanced Diagnosis and Control Laboratory at NC State University. He has published one book, several book chapters, and more than two hundred journal and conference articles. He is an IEEE Fellow, a Co-Editor-in-Chief of IEEE Trans. on Industrial Informatics, Editor-in-Chief of *IEEE Transactions on Industrial Electronics* 2010-2012. He has received the IEEE Region-3 Joseph M. Biedenbach Outstanding Engineering Educator Award, the IEEE ENCS Outstanding Engineering Educator Award, the IEEE ENCS Service Award, the IEEE Industrial Electronics Society Anthony J Hornfeck Service Award. He is a Distinguished Lecturer of IEEE IES.